Static and Dynamic Analysis of IGBT Power Modules for Low and High-Power Range Electric Drives

A. Bharathsimha Reddy, S. N. Mahato, and Nilanjan Tewari

1 Introduction

Conduction and switching losses are the most significant losses in IGBT for medium and high-power applications. The life cycle of the power device will also be affected by the junction temperature of the IGBT [1]. This information will aid in the development of gate drive circuits and the prevention of avoidable errors in power electronic applications [2, 3]. The dynamic and static properties of the IGBT have been examined in this study and the important information for designing the gate drive circuit and fabricating power electronic equipment has been given [4–7]. The dynamic behavior of a high-power IGBT module is investigated in this research under various operating situations. In the studies, single pulse tests are utilized to examine the switching way of IGBT and body diodes under a variety of operating situations. A variety of gate-driving approaches for IGBT modules are investigated. Switching transients at different dc-link voltages and junction temperatures are also used to determine the IGBT modules' switching losses. The static and dynamic analysis of the IGBT has been discussed in depth in Sects. 2 and 3, respectively.

A. Bharathsimha Reddy (✉) · S. N. Mahato
NIT Durgapur, Durgapur, West Bengal, India
e-mail: abr.21ee1101@phd.nitdgp.ac.in

N. Tewari
VIT, Chennai, Tamil Nadu, India

S. Kumar et al. (eds.), *Recent Advances in Power Electronics and Drives*,
Lecture Notes in Electrical Engineering 973,
https://doi.org/10.1007/978-981-19-7728-2_9

2 Static Analysis

When the IGBT is switched-on, the V_{CE} fluctuates with the I_C, V_{GE}, and T_j. In the ON state, the V_{CE} signifies a collector emitter voltage drop that is used to calculate the IGBT's power dissipation loss. The lower the V_{CE} value, the smaller the power dissipation loss [8, 9]. As a result, the V_{CE} value of the IGBT must be as low as possible. The *V-I* characteristics of the IGBT is shown in Fig. 1.

V_{GE} should be kept at 15 V and collector current should be kept at or below the rated I_C current.

2.1 ON State

There are two distinctive curve sections in the forward on mode "V_{CE}" and +ve "I_C".

The turn-on and turn-off characteristics of the IGBT are discussed in [10].

The forward transconductance (g_{fs}) is a measurement of the transfer behavior seen in Fig. 1a.

$$g_{fS} = \frac{\Delta I_C}{\Delta V_{GE}} = \frac{\text{“}I_C\text{”}}{\text{“}V_{GE}\text{”} - \text{“}V_{GE(th)}\text{”}}$$

From above g_{fs}, α, I_C [$g_{fS} \alpha I_C$] decrease as chip temp rises [10]. The active region is only run through during switch-on and switch-off in the mode of the switching that is only permitted for power module's functioning with numerous IGBT chips linked in parallel. In this region, stationary module operation is not permitted since $V_{GE(th)}$

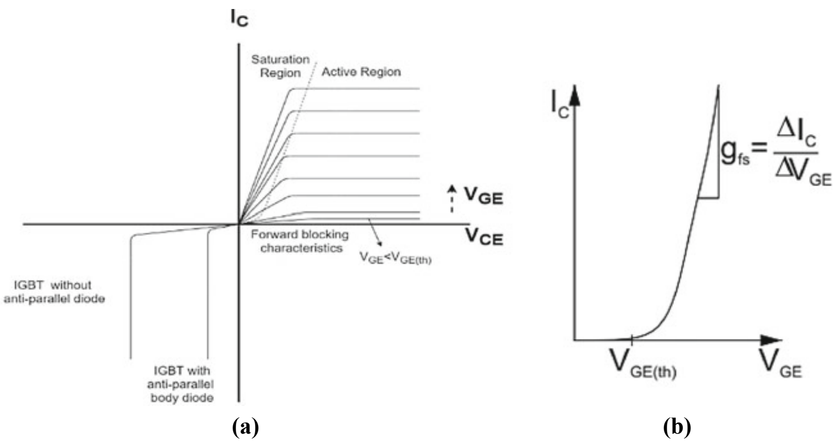

Fig. 1 **a** General static characteristics of the IGBT. **b** Transfer characteristics $I_C = f(V_{GE})$

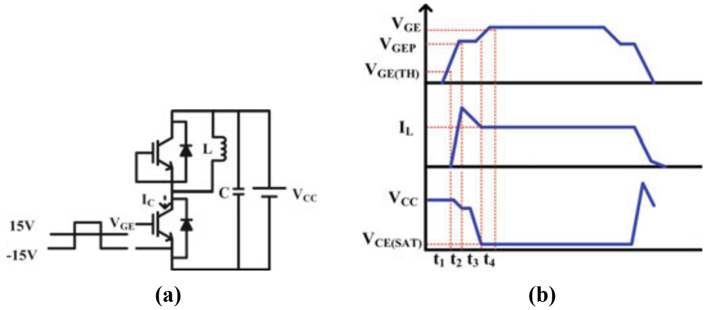

Fig. 2 **a** Switching characteristics measuring circuit. **b** Typical current and voltage waveforms of the IGBT during turn on and turn off

decreases as the temperature rises. This will cause the instability in temperature in each chip.

Saturation region:

The saturation area which corresponds to the ON-state during switching processes has been reached when the I_C is exclusively controlled by the outside circuit. The $V_{CE(sat)}$ of IGBT characterizes the on-state behavior (Fig. 2).

3 Dynamic Analysis of an IGBT Power Module

As the IGBT is so widely used for switching, it's critical to understand both the "turn-on" and "turn-off" switching characteristics in order to calculate "switching-loss". It's also worth remembering that while determining operating conditions, a variety of factors impact these features. The circuit depicted in Fig. 3a has been used to measure the four switching time parameters, *tr*, *ton*, *tf*, and *toff*, as illustrated in Fig. 3b.

The structure, internal capacitances, and internal and external resistances of IGBT power modules impact their switching behavior.

Internal resistances and capacitances influence/effects the IGBT's switching behavior. "C_{GC}" is low and near to "C_{CE}" when the IGBT is off. When V_{GE} surpasses the collector-emitter voltage during the on-state, "C_{GC}" quickly increases. Inversion in the enhancing layer directly under the gate regions causes this quick surge (Table 1).

Since the input and reverse transfer capacitance would grow dramatically in a fully switched transistor, this data can only be used to a limited degree to determine switching behavior.

The charging and discharging rates of the parasitic capacitances are determined by gate resistance. This will affect the IGBT's turn-on and turn-off times.

$$\tau = RC$$

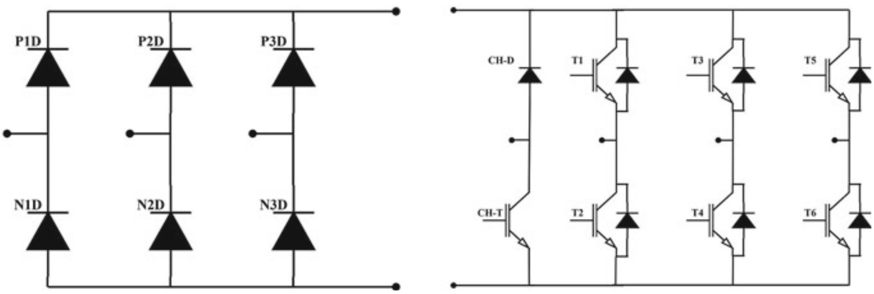

Fig. 3 Power module circuit diagram

Hard switching:

Hard switching occurs when both "I_C" and "V_{CE}" are high for a brief period of time between turn-on and turn-off. This is owing to the fact that a body diode in the load side prevents the current from shutting off as a response of the L_{load}.

IGBTs, unlike any other type of thyristor, can manage these states of operations without the use of passive snubber/filter circuits because of the "dynamic" junction that forms in the drift area during the switching conditions. However, with an IGBT, a significant portion of energy is dissipated during switching states.

$$E_{on,} E_{off} = \int v.idt$$

4 Hardware Implementation and Results

Static test is performed on 50 A, 600 V IGBT Power module. In this test, "$V_{CE(SAT)}$", $V_{GE(th)}$, Forward Voltage drop of Diode (V_F), Collector leakage Current I_{CES}, $I_{GES,}$ and diode (I_R) are measured at 25 and 150 °C (Fig. 4).

4.1 Static Analysis

VCE Measurement at 25 and 150 °C: $V_{CE(SAT)}$ measurements for three IGBT Power module samples S_1, $S_{2,}$ and S_3 are shown in Tables 2 and 3 at 25 °C and 150 °C, respectively. Figures 5 and 6 show the graphical representation of VCE measurements at different gate voltages at 25 °C and 150 °C, respectively.

It is seen from the tables and graphs that when junction temperature rises, so does VCE sat, and vice versa. Furthermore, by lowering the gate voltage, $V_{CE(SAT)}$

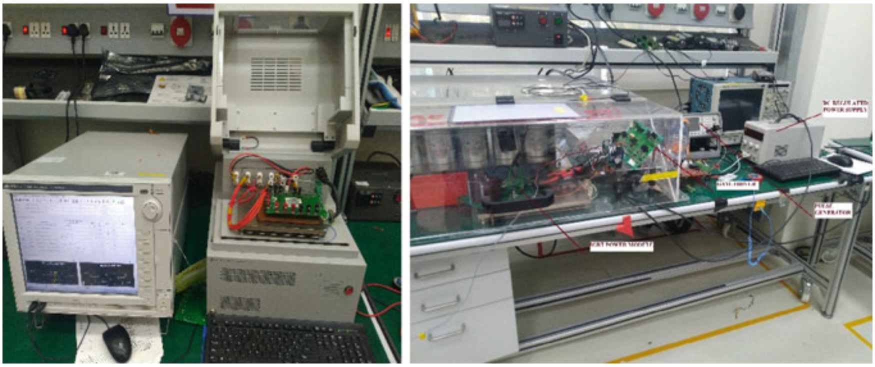

(a) (b)

Fig. 4 **a** Static analysis setup. **b** Dynamic analysis setup

Table 1 Low signal capacitances of IGBT

	IGBT
C_{input}	$C_{ies} = C_{GC} + C_{GE}$
C_{miller}	$C_{res} = C_{GC}$
C_{output}	$C_{oes} = C_{CE} + C_{GC}$

Table 2 V_{CE} measurement at 25 °C

$V_{CE(SAT)}$: $I_{CE} = 50$ A, $V_{GE} = 15$ V, $T_j = 25$ °C							
Initial measurements							
Sample	T_1	T_2	T_3	T_4	T_5	T_6	*CH-T*
S_1	1.81	1.82	1.85	1.82	1.86	1.88	1.96
S_2	1.95	1.99	1.89	2.05	2.01	2.08	2.02
S_3	1.95	1.95	1.99	1.84	1.99	2.01	2.08
Unit = volt							

Table 3 V_{CE} measurement at 150 °C

$V_{CE(SAT)}$: $I_{CE} = 50$ A, $V_{GE} = 15$ V, $T_j = 150$ °C							
Initial measurements							
Sample	T_1	T_2	T_3	T_4	T_5	T_6	*CH-T*
S_1	2.14	2.27	2.3	2.39	2.27	2.32	2.46
S_2	2.19	2.19	2.3	2.3	2.21	2.31	2.46
S_3	2.26	2.25	2.33	2.28	2.36	2.26	2.43
Unit = volt							

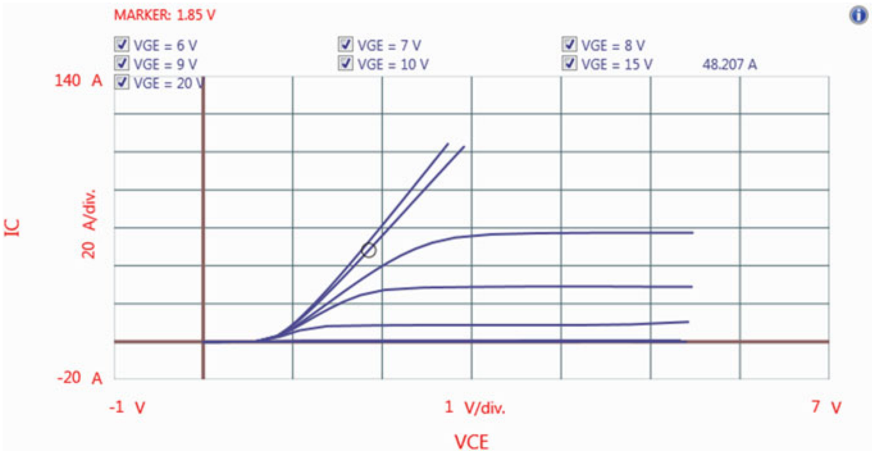

Fig. 5 Graphic plot of $V_{CE(SAT)}$ at 25 °C

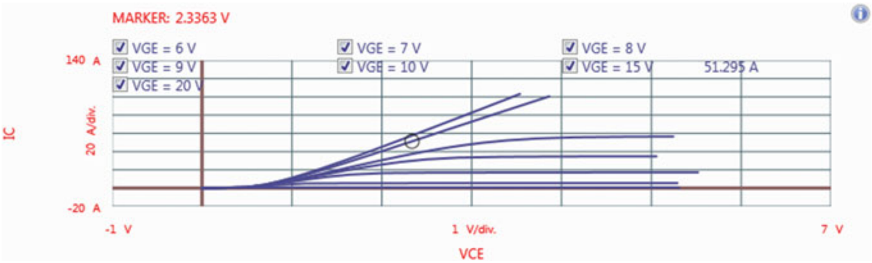

Fig. 6 Graphic plot of $V_{CE(SAT)}$ at 150 °C

will rise. The junction temperature can be managed with the right gate voltage and $V_{CE(SAT)}$. As a result, the power module's life expectancy will be extended.

$V_{GE(th)}$ measurement at 25 and 150 °C: Tables 4 and 5 provide $V_{GE(th)}$ measurements for three IGBT Power module samples S_1, S_2, and S_3 at 25 °C and 150 °C, respectively. Figures 7 and 8 exhibit graphical representations of $V_{GE(th)}$ measurements at various gate voltages at 25 °C and 150 °C, respectively.

The gate-emitter threshold voltage will drop as the temperature rises in the IGBT junction, as shown in the tables and figures above. Breakdown at the gate-emitter junction may occur as a result of this.

VF measurement of body diode at 25 and 150 °C: Tables 6 and 7 show V_f measurements of three IGBT Power module samples S_1, S_2, and S_3 at 25 °C and 150 °C, respectively. Figures 9 and 10 exhibit graphical representations of V_f measurements at various gate voltages at 25 °C and 150 °C, respectively.

The V_F drop of the body diode has increased as the junction temperature (T_j) increases.

Table 4 $V_{GE(th)}$ measurement at 25 °C

$V_{GE(th)}$: $I_c = 0.8$ mA, $V_{GE} = V_{CE}$, $T_j = 25$ °C							
Initial measurements							
Sample	T_1	T_2	T_3	T_4	T_5	T_6	*CH-T*
S_1	5.94	5.91	5.96	5.91	5.91	5.89	5.85
S_2	5.93	5.97	5.95	5.96	5.96	5.96	5.93
S_3	5.92	5.88	5.91	5.91	5.92	5.96	5.88
Unit = volt							

Table 5 $V_{GE(th)}$ measurement at 150 °C

$V_{GE(th)}$: $I_c = 0.8$ mA, $V_{GE} = V_{CE}$, $T_j = 150$ °C							
Initial measurements							
Sample	T_1	T_2	T_3	T_4	T_5	T_6	*CH-T*
S_1	3.86	3.63	3.72	3.59	3.61	3.56	3.31
S_2	3.17	3.36	3.57	3.31	3.18	3.26	3.28
S_3	3.82	3.7	3.82	3.49	3.88	3.79	3.66
Unit = volt							

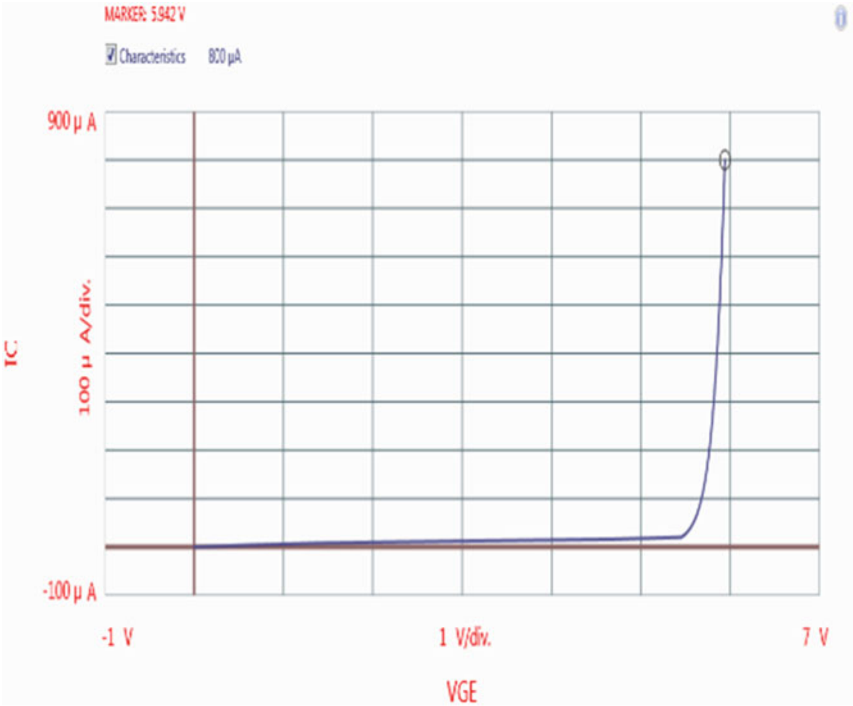

Fig. 7 Graphic plot of $V_{GE(th)}$ at 25 °C

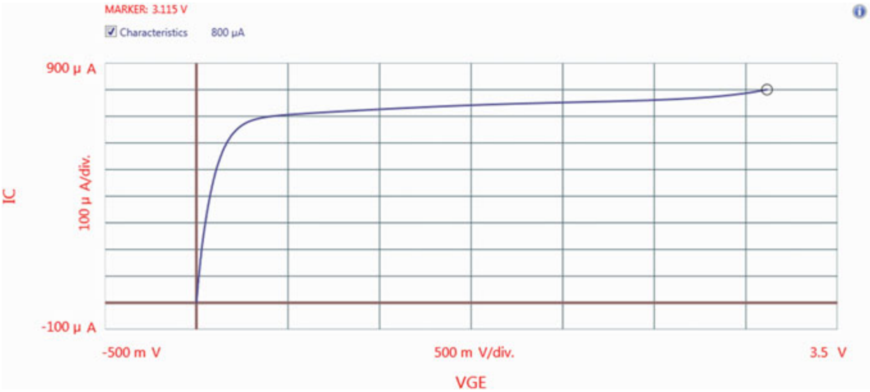

Fig. 8 Graphic plot of $V_{GE(th)}$ at 150 °C

Table 6 V_f measurement at 25 °C

$V_F, I_F = 50$ A for D_1–D_6, $T_j = 25$ °C						
Initial measurements						
Sample	D_1	D_2	D_3	D_4	D_5	D_6
S_1	1.95	1.82	1.85	1.82	1.86	1.88
S_2	2.13	2.16	2.04	2.22	2.17	2.17
S_3	2.12	2.11	2.13	2.26	2.17	2.24
Unit = volt						

Table 7 V_f measurement at 150 °C

$V_F, I_F = 50$ A for D_1–D_6, $T_j = 150$ °C						
Initial measurements						
Sample	D_1	D_2	D_3	D_4	D_5	D_6
S_1	1.89	2.01	2.03	2.12	2.02	2.11
S_2	1.94	1.96	2.03	2.06	1.97	2.12
S_3	2.04	2.02	2.08	2.08	2.14	2.11
Unit = volt						

I_{CE} measurement at 25 and 150 °C: I_{CES} measurements for three IGBT Power module samples S_1, S_2, and S_3 are shown in Tables 8 and 9 at 25 °C and 150 °C, respectively.

I_{CE} measurement at 25 and 150 °C: I_{GES} measurements for three IGBT Power module samples S_1, S_2, and S_3 are shown in Table 10 and Table 11 at 25 °C and 150 °C, respectively.

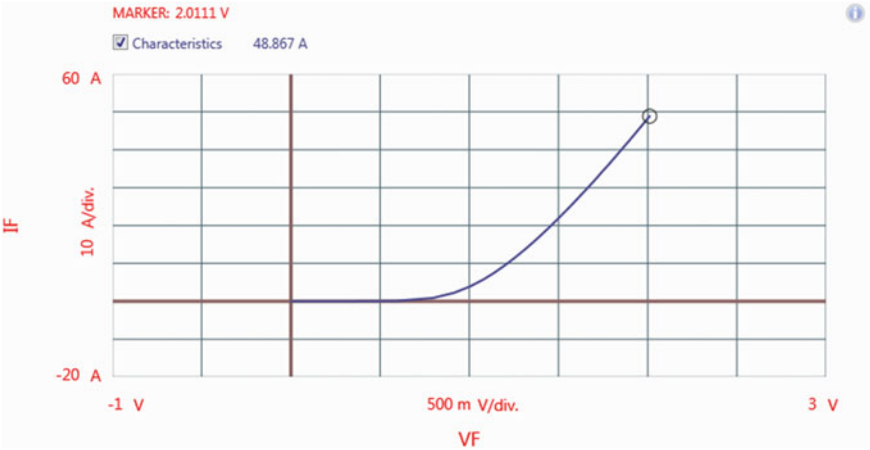

Fig. 9 Graphic plot of V_f at 25 °C

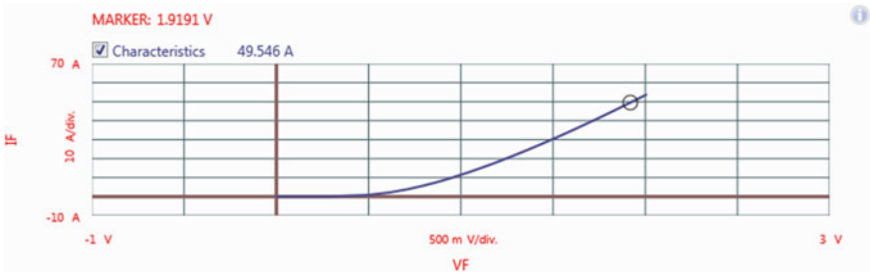

Fig. 10 Graphic plot of V_f at 150 °C

Table 8 I_{CES} measurement at 25 °C

I_{CES}: $V_{CE} = 600$ V, $V_{GE} = 0$, $T_j = 25$ °C							
Initial measurements							
Sample	T_1	T_2	T_3	T_4	T_5	T_6	*CH-T*
S_1	5.94	5.91	5.96	5.91	5.91	5.89	5.85
S_2	5.93	5.97	5.95	5.96	5.96	5.96	5.93
S_3	5.92	5.88	5.91	5.91	5.92	5.96	5.88
Unit = nA							

According to the static analysis, the gate voltage and junction temperature have an impact on the performance of IGBT. For example, lowering the gate voltage raises the junction temperature, which raises the leakage current and the voltage. The gate's threshold voltage is reduced as the junction temperature rises.

Table 9 I_{CE} measurement at 150 °C

I_{CES}: V_{CE} = 600 V, V_{GE} = 0, T_j = 150 °C							
Initial measurements							
Sample	T_1	T_2	T_3	T_4	T_5	T_6	*CH-T*
S_1	0.966	1.15	1.14	1.18	1.17	1.2	1.33
S_2	1.344	1.344	1.324	1.367	1.404	1.374	1.566
S_3	0.980	1.0501	0.965	1.281	0.973	1.0254	1.2102
Unit = nA							

Table 10 I_{GES} measurement at 25 °C

I_{GES}: V_{GE} = ±20 V, T_j = 25 °C							
Initial measurements							
Sample	T_1	T_2	T_3	T_4	T_5	T_6	*CH-T*
S_1	96.1	98	99	96	115	106	160
S_2	105	167	96.5	184	89.5	164	144
S_3	83	109	81.7	124	108	138	101
Unit = pA							

Table 11 I_{GES} measurement at 150 °C

I_{GES}: V_{GE} = ±20 V, T_j = 150 °C							
Initial measurements							
Sample	T_1	T_2	T_3	T_4	T_5	T_6	*CH-T*
S_1	280	303	255	255	908	247	231
S_2	246	338	190	324	203	222	301
S_3	298	395	179	2.67n	4.44n	948	101
Unit = pA							

4.2 Dynamic Analysis

Dynamic analysis was performed in three different gate resistances of 3.5, 12, and 22 Ω, as well as at 25 and 125 °C (Figs. 11, 12, 13 and 14).

From the dynamic analysis, it is seen that the switch-on time, switch-off time, and blanking time are all determined by the R_g of the IGBT. From Tables 12 and 13, it is found that when gate resistance is low, the IGBT's on and off times are shorter. The IGBT takes longer time to switch on and off when the gate resistance is large.

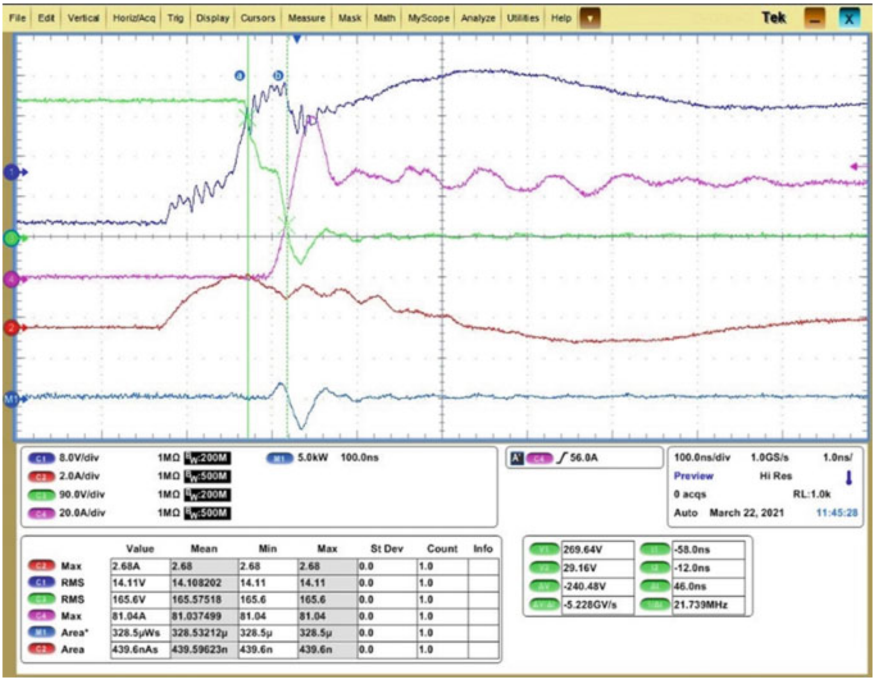

Fig. 11 Turn on wave form with $R_g = 3.5\ \Omega$ at 25 °C

When gate resistance is high, charging and discharging of C_G is slow; when gate resistance is low, charging and discharging of C_G is quick. When gate resistance is low, the voltage and current fluctuations with respect to time are greater, and when gate resistance is more, the voltage and current variations with respect to time are less. From Tables 12 and 13, it is understood that the value of the gate resistance is having impact on peak current, peak voltage, and reverse recovery characteristics of the IGBT.

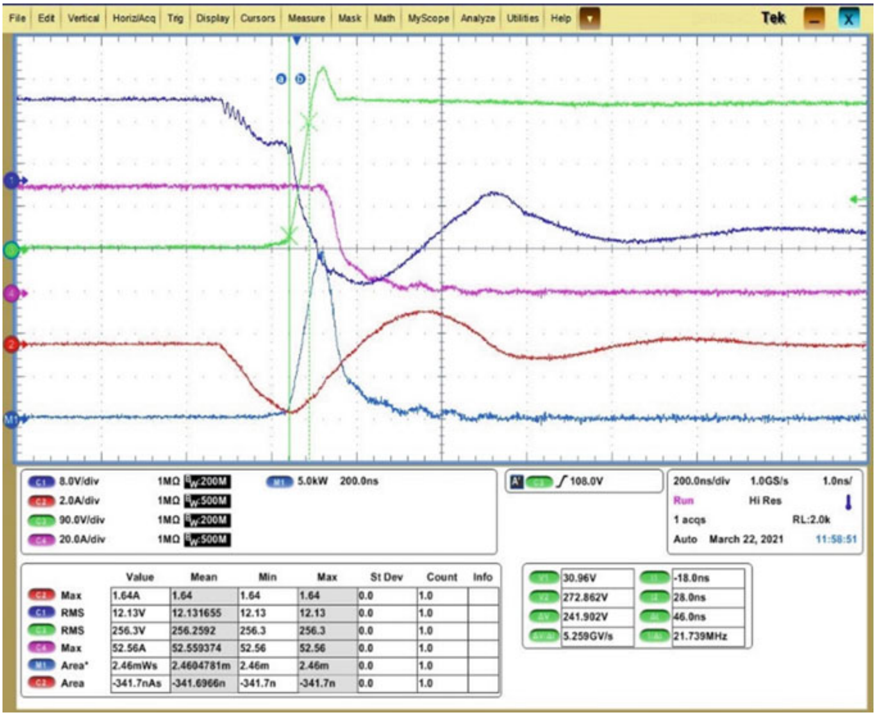

Fig. 12 Turn off wave form with $R_g = 3.5\ \Omega$ at 25 °C

The dynamic test was carried out at two distinct temperatures (25 and 125 °C). The energy loss is greater when the ambient temperature reaches 125 °C according to the test. The reverse recovery time is influenced by the ambient temperature. When the ambient temperature is higher, the reverse recovery period is longer.

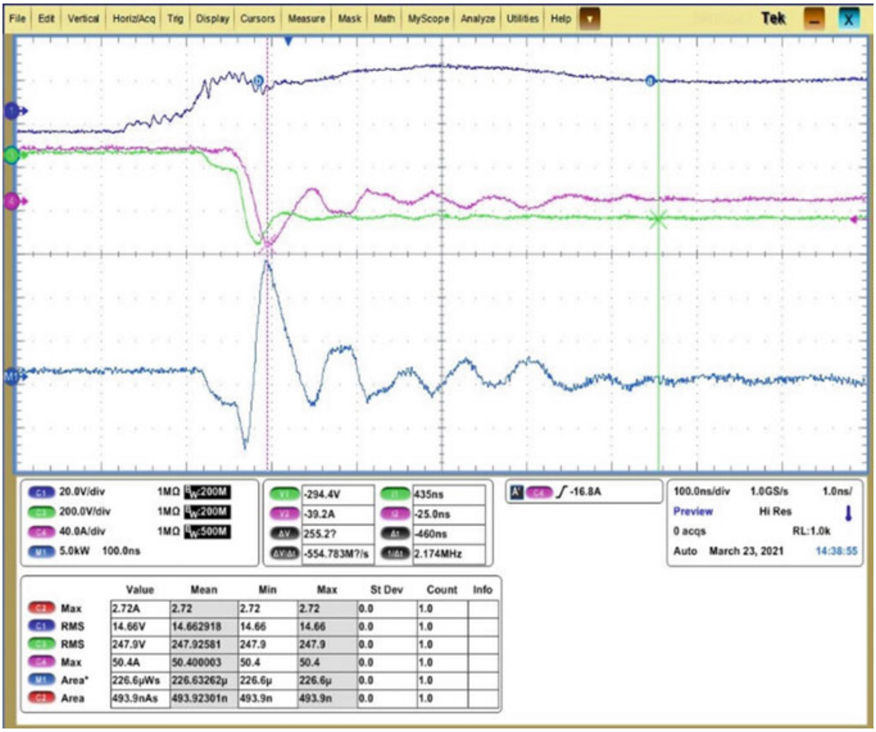

Fig. 13 Turn on wave form with $R_g = 3.5\ \Omega$ at 125 °C

5 Performance Analysis with Respect to Speed

The efficiency of electric drives is entirely dependent on the motor's speed and torque. When the drive operates at low speed and torque, the efficiency is reduced. Table 14 shows a comprehensive study of the drive at various speeds and torques. It is found that raising the speed and torque till the rated values increases the efficiency of the drive.

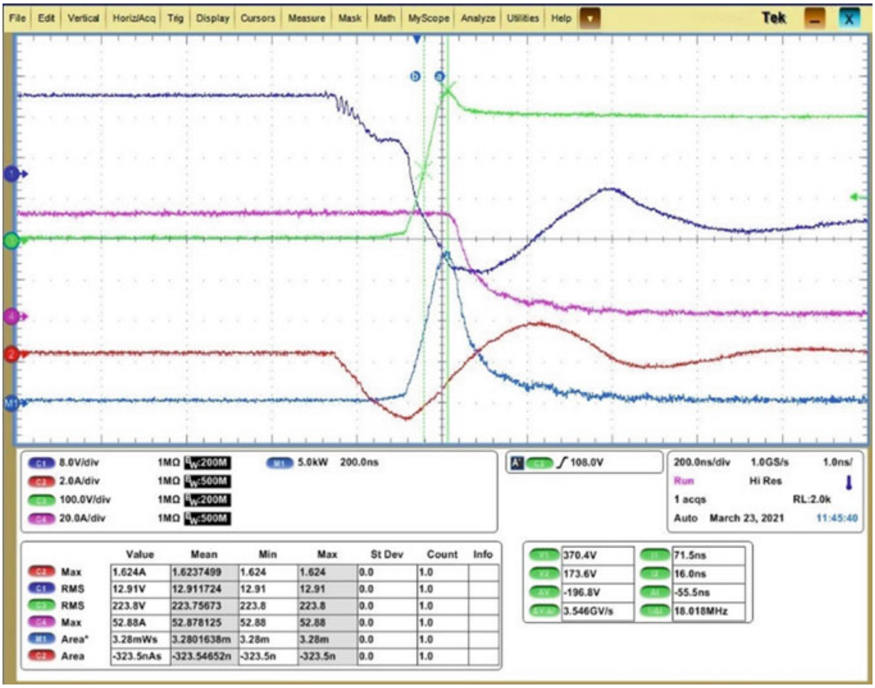

Fig. 14 Turn off wave form with $R_g = 3.5\ \Omega$ at 125 °C

6 Conclusion

The influence of the gate resistance on circuit characteristics is first examined in this study. Based on the discussions, some recommended resistor values have been determined for various applications, which can be used as a starting point for optimization. In any case, the final value is utilized to test the circuit in concern. Simultaneously, an example on how to pick appropriate drive modules for the determined R_g value is shown. Finally, several circuit layout methodologies and concepts have been discussed in brief. Total losses are minimized by maintaining the optimum saturation voltage across the collector and the emitter and the rated gate voltages. This information might be useful to the circuit designers. The junction temperature, gate

Table 12 Dynamic test results at 25 °C

25 °C				
	R ohms	3.5	12	22
Energy loss	*Eon* mJ	0.3285	0.2949	1.288
	Eoff mJ	2.826	2.246	2.335
Gate charge	*Qg* on nC	439.6	340	330.2
	Qg off nC	−338.9	−363.7	−345.3
Reverse recovery	*Err* mJ	0.2266	0.3394	0.093
	Qrr nC	493.9	491.9	585.3
Time	*trr* ns	54	58	132
	tr ns	22.5	31.4	140
	tf ns	99.5	140	189.5
	tdon ns	44	49.1	74
	td off ns	244	296	408.5
	Ip (A)	81.036	76.4	63.44
	Vp (V)	389.52	377.6	405.6
	Irp (A)	−44.128	−30.8	−15.77
	di/*dt* on	1.826 GA/s	1.25 GA/s	0.78 GA/s
	di/*dt* off	−393 MA/s	−290 MA/s	−0.4 GA/s
	dv/*dt* on	−5.2 GV/s	−3.97 GV/s	−1.3 GV/s
	dv/*dt* off	−5.26 GV/s	5.02 GV/s	3.3 GV/s
	dv/*dtr*	−5.64 GV/s	−5.6 GV/s	−1.7 GV/s

voltage, and gate resistance should all be kept within a certain range for improved IGBT performance, as stated in this work.

Table 13 Dynamic test results at 125 °C

125 °C				
	R ohms	3.5 Ω	12 Ω	22 Ω
Energy loss	*Eon* mJ	0.362	0.432	1.492
	Eoff mJ	3.28	2.248	2.836
Gate charge	*Qg* on nC	416.7	331	326.8
	Qg off nC	−323.5	−368.98	−353.4
Reverse recovery	*Err* mJ	1.34	1.15	0.939
	Qrr nC	493.2	500	344.9
Time	*trr* ns	162	164.5	318.5
	tr ns	24	31.2	57.5
	tf ns	167	171	169.5
	tdon ns	45	53.2	74.5
	td off ns	272	329.5	442.5
	Ip (A)	93.6	94	74
	Vp (V)	370	374.4	383.18
	Irp (A)	−59.4	−49.56	−31.8
	di/*dt* on	1.655 GA/s	1.295 GA/s	699 MA/s
	di/*dt* off	−240 MA/s	−233 MA/s	−241 MA/s
	dv/*dt* on	−3.9 GV/s	−3.1 GV/s	−1.1 GV/s
	dv/*dt* off	3.87 GV/s	3.94 GV/s	2.81 GV/s
	dv/*dtr*	−4.29 GV/s	−4.19 GV/s	−1.44 GV/s

Table 14 Performance of electric drive at various speeds and loads

Test no.	Line voltage (V RMS)	Motor frequency (% of nom. freq)	Load/torque (% of NO)	Output current (A)	Motor speed (RPM)	Input power (kW)	Output power (kW)	Loss (W)	Efficiency (%)
1	400	20	25	16.4	306	1.2	1.056	0.144	88.00
2		20	50	19.6	312	2.24	2.058	0.182	91.88
3		20	75	24	316	3.26	3.018	0.242	92.58
4		20	100	29.3	320	4.3	4	0.3	93.02
5		50	25	16.6	735	2.75	2.58	0.17	93.82
6		50	50	20.5	742	5.13	4.91	0.22	95.71
7		50	75	26.2	747	7.62	7.31	0.31	95.93
8		50	100	31.7	752	9.87	9.47	0.4	95.95
9		100	25	16.6	1466	5.05	4.88	0.17	96.63
10		100	50	21	1471	9.92	9.69	0.23	97.68
11		100	75	27	1478	14.7	14.38	0.32	97.82
12		100	100	33.1	1485	19.9	18.76	1.14	94.27

References

1. N. Chen, F. Chimento, M. Nawaz, L. Wang, dynamic characterization of parallel connected high power IGBT modules. IEEE Trans. Ind. Appl. **51**(1) (2015)
2. Y. Gao, A.Q. Huang, S. Krishnaswami, A.K. Agarwal, Comparison of static and switching characteristics of 1200 V 4H-SiC BJT & 1200 V Si-IGBT. IEEE Trans. Ind. Appl. **44**(3) (2008)
3. R. Alvarez, F. Filsecker, S. Bernet, Characterization of a new press pack SPT + IGBT for medium voltage converters, in *Proceedings of the IEEE ECCE* (2009), pp. 3954–3962
4. R. Letor, Static & dynamic behavior of paralleled IGBT's. IEEE Trans. Ind. Appl. **28**(2) (1992)
5. K. Zou, L. Qi, X. Cui, G. Zhao, B. Zong, The design & measurement of test system for dynamic characteristics of IGBT, in 2014 *International Conference on Power Systems Technology (POWERCON 2014)*, Chengdu, 20–22 Oct. 2014 (2014)
6. S.-W. Hu, Y.-J. Zhu, Y.-Y. Duan, An impact analysis of gate R_g on static and dynamic dissipation of IGBT modules, in *IEEE Conference* (2011). 978-1-4577-0321-8/11
7. C. Wang, Y. He, C. Wang, L. Li, J. Li, X. Wu, Multi-chip parallel IGBT power module failure monitoring based on gate dynamic characteristics, in *IEEE Conference* (2020). 978-1-281-5281-3/20
8. A. Arya, P. Kumar, S. Anand, Methodology of an accurate static I–V characterization of power semiconductor devices. IEEE Trans. Instrum. Meas. **69**(10) (2020)
9. Z. Wang, H. Zhang, J.B. Kuo, Turn-off transient analysis of super junction IGBT. IEEE Trans. Electron. Devices **66**(2) (2019)
10. B. W. Williams, *Power Electronics*